ENGLISH VERSION

Study of fatigue performance in a pavement concrete mix reinforced with steel fibers

Estudio del comportamiento a la fatiga de una mezcla de concreto para pavimentos reforzada con fibras metálicas

D. Ruiz-Valencia [1]*, F. Rodríguez **, M. León-Neira *

* Pontificia Universidad Javeriana, Bogotá. COLOMBIA
** Holcim (Colombia) S.A. COLOMBIA

Fecha de Recepción: 31/10/2016
Fecha de Aceptación: 03/02/2017
PAG 45-58

Abstract

The behavior in flexural fatigue tests of concrete containing metal fibers has not been extensively studied. Therefore, this study aims at determining the effects of incorporating metal fibers in concrete paving on flexural fatigue tests. A concrete mix was designed with modulus of rupture of 4.1 MPa at 28 days, which was added with steel fibers of 35 mm long and 0.5 mm in diameter in 3 proportions: 20 kg/m^3, 40 kg/m^3 and 80 kg/m^3 and left to a non-corresponding control mixture addition. Fatigue tests were performed on 68 specimens of 100 x 100 x 350 mm, at a frequency of 8 Hz, and stresses between 80% and 90% of the modulus of rupture of each mixture. The Weibull probability distribution was used to calculate the fatigue curves with different failure probabilities. For the stress ranges studied, the fatigue life did not increase in the mix with fiber content of 20 kg/m^3, but it did increase by 6% to 40 kg/m^3 (0.5%) and 25% to 80 kg/m^3 (1%), compared with the control mixture.

Keywords: *Steel fiber reinforced concrete, fatigue tests, pavements*

Resumen

El comportamiento en ensayos de fatiga por flexión de concretos que contienen fibras metálicas no ha sido ampliamente estudiado. Por esta razón, se planteó este estudio para determinar el efecto de la incorporación de fibras metálicas en concretos para pavimentos en ensayos de fatiga por flexión. Se diseñó una mezcla de concreto con módulo de rotura de 4.1 MPa a 28 días, a la cual se le dosificaron fibras metálicas de 35 mm de largo y 0.5 mm de diámetro en tres proporciones: 20 kg/m^3, 40 kg/m^3 y 80 kg/m^3 y se dejó una sin adición correspondiente a la mezcla de control. Los ensayos de fatiga se realizaron sobre 68 especímenes de 100 x 100 x 350 mm, a una frecuencia de 8 Hz, se aplicaron esfuerzos entre el 80% y 90% del módulo de rotura de cada mezcla. Con la distribución de probabilidad Weibull se calcularon las curvas de fatiga con diferentes probabilidades de falla. En los rangos de esfuerzos estudiados, la vida de fatiga no aumenta para contenido de fibras de 20 kg/m^3 y aumenta un 6% para 40 kg/m^3 (0.5%) y 25% para 80 kg/m^3 (1%) comparado con la mezcla control.

Palabras clave: Concreto reforzado con fibras metálicas, ensayos de fatiga, pavimentos

1. Introduction and background

Pavements are structures subjected to cyclic loading imposed by traffic and combined weather effects (Huang Yang, 2004; LCPC, 1997; Packard, 1984; Papagiannakis and Masad, 2008; Reyes, 2003). In concrete pavements, the concrete slab absorbs most of these stresses (Huang Yang, 2004; Packard, 1984) which are mainly compressive and flexural stresses (Huang Yang, 2004; Papagiannakis and Masad, 2008), where the latter is most critical for concrete, since the concrete flexural strength in concrete is lower than the compressive strength (Bentur and Sidney, 2007; Z. Li, 2011; Mehta and Monteiro, 2006). This concrete weakness is compensated by the steel reinforcement, which is incorporated to the concrete through corrugated steel bars (reinforced concrete) or metal fibers (fiber reinforced concrete) (Mehta and Monteiro, 2006). The latter are frequently used with the additional purpose of increasing the fatigue strength (ACI Committee 544, 2009; Bentur and Sidney, 2007; Meda and Plizzari, 2004). Furthermore, they are easy to install and guarantee their dispersion throughout the whole concrete mass (Bentur and Sidney, 2007), something that corrugated steel bars cannot achieve.

The repeated action of flexural stress generates a progressive loss of the structural properties of concrete, a process known as material fatigue (Lee and Barr, 2004; Vassilopoulos, 2010). The mechanistic methods of pavement design use material fatigue laws to determine the capacity of pavement to resist stresses, deformations and deflections imposed by traffic volumes and the weather (Papagiannakis and Masad, 2008). Traditionally, concrete pavement designs use fatigue models such as the PCA model (Portland Cement Association) (Packard, 1984), the MEPDG (Mechanistic Empirical Pavement Design Guide) of the AASHTO (American Association of State Highway and Transportation Officials) (MEPDG, 2007), the mechanistic calibrated model (US Army Corps of Engineers) (Huang Yang, 2004), the French rational method (LCPC, 1997) and the zero maintenance model (Federal Highway Administration) (Huang Yang, 2004). It is important to mention that these models were developed under conditions and with materials

[1] *Corresponding author:*

Profesor Asociado, Director de Departamento de Ingeniería Civil, Pontificia Universidad Javeriana, Bogotá. Colombia
E-mail: daniel.ruiz@javeriana.edu.co

that are not the same as in South American countries. Additionally, they were developed for non-reinforced concrete; therefore, it is necessary to develop fatigue models for non-reinforced concrete and steel fiber reinforced concrete with local materials that allow quantifying the effect of steel fibers in the materials fatigue life.

The interest to address the study of concrete fatigue dates back to the end of the XIX century in the United States, with the construction of reinforced concrete bridges for railways, which studied the concrete fatigue under compressive loading (Hsu, 1981). While the study of the fatigue performance of concrete in flexural tests started together with the development of the US highway system at the beginning of 1920 (Hsu, 1981; Shi, Fwa and Tan, 1993).

Concrete fatigue originates a kind of deterioration in concrete pavements that is evidenced by breaking of the concrete slab, thus generating a water inlet source and the subsequent erosion of the slab supporting material, which leads to the total destruction of the pavement structure (Huang Yang, 2004; Papagiannakis and Masad, 2008).

The concrete's fatigue performance is a relevant parameter in the design of concrete pavements for highways, airports and industrial facilities; therefore, it should be controlled, together with the erosion of the slab supporting materials (Huang Yang, 2004; Packard, 1984; Papagiannakis and Masad, 2008; Shi et al., 1993). The erosion of the supporting material is limited by using water-resistant materials, such as asphalt mixes or poor hydraulic concrete, which increase the stiffness of the concrete slab in order to reduce deflections transmitted to the support, and by using load transfer devices in the discontinuities of the slab (Huang Yang, 2004; Packard, 1984; Papagiannakis and Masad, 2008). In order to control the fatigue process of concrete, it is necessary to know the properties governing the performance of this phenomenon.

The fatigue performance is normally studied in terms of the stress applied, expressed as a percentage of the modulus of rupture (known as stress ratio) against the number of loading cycles applied to the failure (Johnston and Zemp, 1991; Shi et al., 1993). Results are represented in curves known as Whöler curves. In order to eliminate the influence of the water-cement ratio, type and grading of aggregates, and the type and quantity of cement in concrete, researches have chosen to use the stress ratio instead of the rupture stress (Huang and Zhao, 1995; Lee and Barr, 2004; Shi et al., 1993).

In general, parameters like loading conditions, loading frequency, stress level, number of cycles, composition of the matrix and the stress ratio will have an impact on the fatigue performance of the concrete specimen; however, there is no qualitative and quantitative consensus regarding how these parameters impact the fatigue performance of concrete (Lee and Barr, 2004).

Fatigue testing of concrete uses important resources of time and money. Therefore, the design of concrete pavements is commonly based on curves from road organizations, such as those developed by the PCA (Packard, 1984), the MEPDG of AASHTO (MEPDG, 2007), the mechanistic calibrated model (US Army Corps of Engineers) (Huang Yang, 2004), the French rational method (LCPC, 1997) and the FHWA zero maintenance model (Huang Yang, 2004).

Since the French rational method of pavement design characterizes fatigue curves with 2 parameters that are easily obtained, rupture stress for one million loading cycles σ_6 and slope of the fatigue curve b, it allows comparing results reported by different authors. Table 1 shows the parameters of the French rational method of the fatigue curves presented by some authors (Goel et al., 2012; Johnston and Zemp, 1991; Oh, 1991; Shi et al., 1993). These results will be the basis to compare the parameters obtained in this study.

***Table 1.** French rational method parameters for fatigue curves without fibers*

Author	Range evaluated in stress ratios		MR (MPa)	σ_6 (MPa)	b	-1/b	σ_6/MR
Byung Hwan, 1991	65%	85%	4.54	2.80	-0.052	20	0.62
Johnston et al., 1991	80%	90%	4.45	3.20	-0.040	25	0.72
Shi et al., 1993	65%	90%	6.04	3.50	-0.042	24	0.58
Goel et al., 2012	65%	90%	4.89	3.10	-0.045	23	0.63
LCPC - SETRA, 1997 (Clase 5)				2.15	-0.063	16	
LCPC - SETRA, 1997 (Clase 4)				1.95	-0.067	15	
LCPC - SETRA, 1997 (Clase 3)				1.63	-0.067	15	
LCPC - SETRA, 1997 (Clase 2)				1.37	-0.071	14	
PCA, 1984	45%	100%					0.50

2. Methodology

In order to meet the objectives of this study, a physical and chemical characterization of the gravel, sand and cement was made. These materials were used in the design of a concrete pavement mixture, according to the ACI-211.1 method, that would comply with a minimum flexural strength of 4.1 MPa at 28 days and slump at 125 mm. Concrete mixtures with steel fiber contents of 20 kg/m³, 40 kg/m³, 80 kg/m³, and plain control mixes were manufactured. Each mixture in the plastic state was subjected to slump, air content and unit mass tests. In the hardened state, compressive strength and modulus of elasticity were measured in cylinders of 150 mm diameter and 300 mm height, and the modulus of rupture, in beams of 150 mm x 150 mm x 550 mm. Flexural fatigue tests were carried out in a MTS dynamic system, on specimens measuring 100 mm x 100 mm x 350 mm. The load was applied at the middle third of the clear span and magnitudes were 90% and 80% of the maximum load of the modulus of rupture. Dynamic loading was applied at a speed of 8 Hz and the ratio between minimum stress and maximum stress applied by loading cycle was set at 0.01. Loading cycles tested to rupture at each loading stress applied were statistically processed to adjust them to a Weibull distribution function and thus incorporate parameters of failure probability to predict loading cycles to rupture for a specific failure probability. These values were used to draw fatigue curves and calculate rupture stresses for one million loading cycles (σ_6) and the slopes of fatigue laws b.

2.1 Physical and chemical characterization of the materials and mix design

The materials for producing the concrete used in the fatigue tests were based on their compliance with the requirements of the specification No. 600-11 of the Urban Development Institute of Bogota, Colombia. Gravels and sands came from an alluvial source of the Department of Tolima.

The cement used was type 1M (according to the Colombian Standard NTC-30), with 15% slag addition, which complies with NTC-4018. The cement tests are those mentioned in the standards NTC-121 and NTC-321. The water used for mixing and curing the samples comes from the Bogota D.C. aqueduct for human consumption. Two additives were used, a high-range plasticizer and a water reducer, which comply with NTC-1299 and ASTM C-494, respectively. These additives were not subjected to control tests, since they were delivered with certification from the supplier. The metal fibers were made of cold-drawn low carbon steel, non-galvanized, whose tensile strength, according to the manufacturer's report, is 1100 MPa; they were 35 mm long with a diameter of 0.55 mm and the ends were bent in the form of a hook. Fibers were joined by an adhesive that melted when entering into contact with the mixing water. These fibers were manufactured according to the ASTM-A820 specification.

The concrete mix design followed the procedure of ACI-211.1. As input data for the concrete mix design, a flexural strength of 4.1 MPa at 28 days with a slump of 125 mm was established. This concrete strength considered the fact that it is the most used in pavement construction in the city of Bogota. It should be noted that, in the ACI-211.1 procedure, the input data is the compressive strength; therefore, equation 1 was used, which expresses a correlation taken from the Colombian regulations for earthquake-resistant construction (2010).

$$MR = 0.62\sqrt{f'c} \qquad (1)$$

Where, MR is the required modulus of rupture in MPa and f'c is the required compressive strength in MPa. The fiber quantities considered for manufacturing the specimens were 20 kg/m³, 40 kg/m³ and 80 kg/m³. These proportions were set to cover from the minimum required by the manufacturer of the fiber to twice the maximum recommended by the manufacturer of the fiber. Moreover, control samples without fibers were made to quantify the variations in the studied properties.

Table 2. *Indicates the tests carried out with gravels and sands*

Gravel and Sand Tests	Test Standard
Petrographic Analysis	ASTM C-295
Grading	INV E-213-07
Los Angeles Abrasion	INV E-218-07
Micro-Deval	INV E-238-07
10% fine aggregates	INV E-224-07
Losses in sulfate soundness test (magnesium)	INV E-220-07
Clay clods and poor particles	INV E-211-07
Light particles	INV E-221-07
Mechanically fractured particles	INV E-227-07
Flatness Index	INV E-230-07
Elongation Index	INV E-230-07
Sulfate content	INV E-233-07
Liquid Limit*	INV E-125-07
Plasticity Index*	INV E-126-07
Sand Equivalent*	INV E-133-07
Methylene blue value*	INV E-235-07
Material passing sieve 75µm (No.200)*	INV E-214-07
Organic matter*	INV E-212-07
Water absorption*	INV E-222-07
Reactivity	INV E-234-07

2.2 Tests in the plastic state and mechanical tests in the hardened state

The laboratory test program established two moments of the concrete mixture; the first corresponds to the plastic state or freshly mixed, and the second to the hardened state of the mix at different ages. Tests were run for concrete in the plastic state, as shown in Table 3, and in the hardened state in Table 4.

Slump tests of concrete reinforced with fibers followed the procedure of the NTC-396 and not the ASTM-C995, considering the indications of the ACI-544 Committee (quoted by Bentur and Sidney, 2007), which states that once a satisfactory handling is achieved with a fiber reinforced concrete, and the control has been made with the slump test, the latter can be used to monitor the consistency of the fiber-reinforced mixture. This allowed keeping a comparison parameter with the control sample.

2.3 Fatigue tests

Fatigue tests were carried out on prismatic specimens of 100 mm x 100 mm x 350 mm. Prior to the test, these specimens underwent a curing process immersed in water under controlled conditions, according to NTC-550. Consequently, at the time of the fatigue test, specimens were moist.

Then, it was verified that the minimum dimension was 3 times bigger than the maximum gravel size, which was 25 mm, so the minimum dimension should be 75 mm. However, considering that the length of the steel fiber was 35 mm, this dimension was extended to 100 mm to avoid being orientated in the sense of the fibers.

The number of manufactured joists was 96, from which 28 were tested in the static mode (monotonic loading) to obtain the modulus of rupture of the prismatic beams of 100 mm x 100 mm x 350 mm, and 68 were tested in the dynamic mode (cyclic load) to find the number of loading cycles to failure. In order to obtain the modulus of rupture in the prismatic beams of 100 mm x 100 mm x 350 mm, a monotonic load was applied at a standardized speed of 1 MPa/min until rupture.

Once the rupture under load was obtained, this value was used for finding the reference load for the specimens subjected to fatigue, which corresponds to 90% to 95% and 80 to 85% of the rupture under load. Specimens were subjected to a controlled stress-loading mode applied at the third points of the span at a frequency of 8 Hz. The ratio between the minimum stress and the maximum stress applied by loading cycle was set at 0.01.

The equipment used for the fatigue tests was a MTS system with loading capacity of 100 kN.

Table 3. *Tests of freshly mixed concrete*

Fresh Concrete Tests	***Test Standard***
Concrete slump	*NTC-396*
Unit mass	*NTC-1926*
Air content	*NTC-1032*

Table 4. *Tests of hardened concrete*

Hardened Concrete Tests	**Test Standard**
Plain compressive strength of cylinders	NTC-673
Flexural strength of concrete (loading at third points of the span)	NTC-2871
Modulus of elasticity of concrete	NTC-4025

2.4 Statistical analysis of results

Fatigue results were processed with the Weibull probability distribution, considering the indications of Gumble (quoted by Singh and Kaushik, 2000), who mentioned that the hazard function of the lognormal distribution decreases as time or life increases.

In order to obtain the Weibull probability distribution function, it is necessary to find the shape parameters of function (α) and the scale parameter (μ), based on Equations 2 and 3.

$$\alpha = (COV)^{-1.08} \quad (2)$$

Where, COV is the coefficient of variation of the number of cycles to failure under a specific load.

$$u = \frac{\mu}{Gamma\left(\frac{1}{\alpha}+1\right)} \quad (3)$$

In equation 3, μ is the average of the number of cycles to failure under load; Gamma is the statistical function, and α was previously defined.

Equation 4 was adopted to include the failure probability (P) in the calculation of the number of cycles to failure under load, according to the model proposed by Singh and Kaushik (2000):

$$n = ln^{-1}\left(\frac{ln\left(ln\left(\frac{1}{1-P_f}\right)\right)+\alpha ln\,(u)}{\alpha}\right) \quad (4)$$

Where n is the number of cycles to failure under a load applied for failure probability. For each curve, the rupture stress for one million loading cycles (σ_6) and the slope of the fatigue law b were calculated.

3. Results and discussion

The results of the execution of each of the activities defined in the work methodology are described below.

3.1 Physical and chemical characterization of the materials and mix design

Table 5 shows the results of the gravel tests. Figure 1 shows the obtained grading.

Table 5. *Gravel test results*

Gravel Tests	Test Standard	Requirement	Result
Petrographic Analysis	ASTM C-295	Reactive Minerals	None
Los Angeles Abrasion	INV E-218-07	Max. 30%	23.4%
Micro-Deval	INV E-238-07	Max. 25%	22.7%
10% fine aggregates	INV E-224-07	Min. 75 kN	274
Moist/Dry Ratio	INV E-224-07	Min. 75%	95%
Losses in sulfate soundness test (magnesium)	INV E-220-07	Max. 18%	4.2%
Clay clods and poor particles	INV E-211-07	Max. 0.25%	0.03%
Light particles	INV E-221-07	Max. 1%	0%
Mechanically fractured particles – 1 face	INV E-227-07	Min. 85%	100%
Mechanically fractured particles – 2 faces	INV E-227-07	Min. 70%	100%
Flatness Index	INV E-230-07	Max. 20%	17%
Elongation Index	INV E-230-07	Max. 20%	19%
Sulfate content	INV E-233-07	Max. 1%	0.0001%
Reactivity	INV E-234-07	Non-reactive	Non-reactive

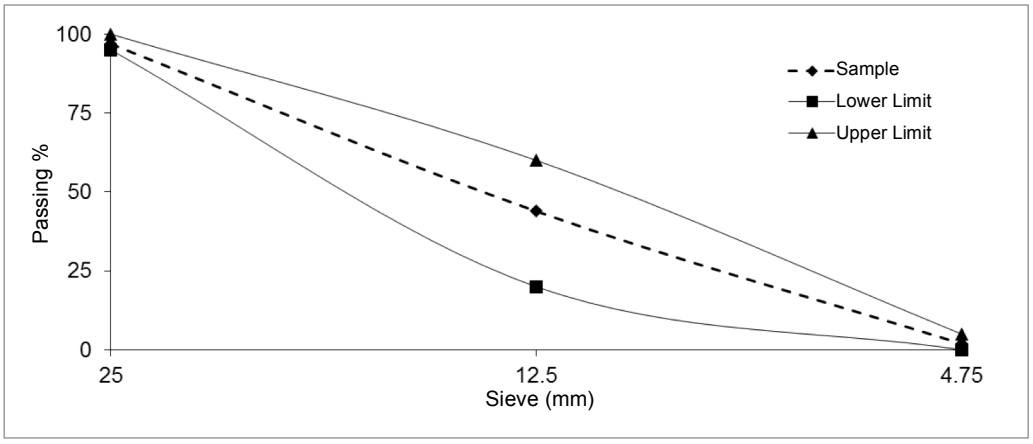

Figure 1. *Gravel grading – IDU 600-11 specification limits*

Table 6 shows the results of the sand tests and Figure 2 indicates the obtained grading.

Table 7 shows the results of the chemical tests in cement and Table 8 shows results of the physical and mechanical tests in cement.

The concrete mix design followed the procedure of ACI-211.1, which was adjusted with a water reducer additive (0.45% of the cement weight) and a high-range plasticizer (0.15% of the cement weight). The proportion of the additives followed the recommendation of the manufacturer. The proportions used in the concrete mix are indicated in Table 9.

The design verification was made by testing beams of 150 mm x 150 mm x 550 mm at 3 days, 7 days and 28 days, and the results are shown in Figure 3.

Table 6. *Sand test results*

Sand Tests	Test Standard	Requirement	Result
Petrographic Analysis	ASTM C-295	Reactive Minerals	None
Losses in sulfate soundness test (magnesium)	INV E-220-07	Max. 15%	6%
Liquid limit	INV E-125-07	Non-plastic	Non-plastic
Plasticity index	INV E-126-07	Non-plastic	Non-plastic
Sand equivalent	INV E-133-07	Min. 50%	63%
Methylene blue equivalent	INV E-235-07	Max. 5%	2%
Clay clods and poor particles	INV E-211-07	Max. 1%	0.5%
Light particles	INV E-221-07	Max. 0.5%	0%
Material passing sieve of 75µm (No.200)	INV E-214-07	Max. 5%	4.69%
Organic matter	INV E-212-07	Max. plate No.3	Plate No.1
Sulfate content	INV E-233-07	Max. 1.2%	0%
Reactivity	INV E-234-07	Non-reactive	Non-reactive
Water absorption	INV E-222-07	Max. 4%	1%

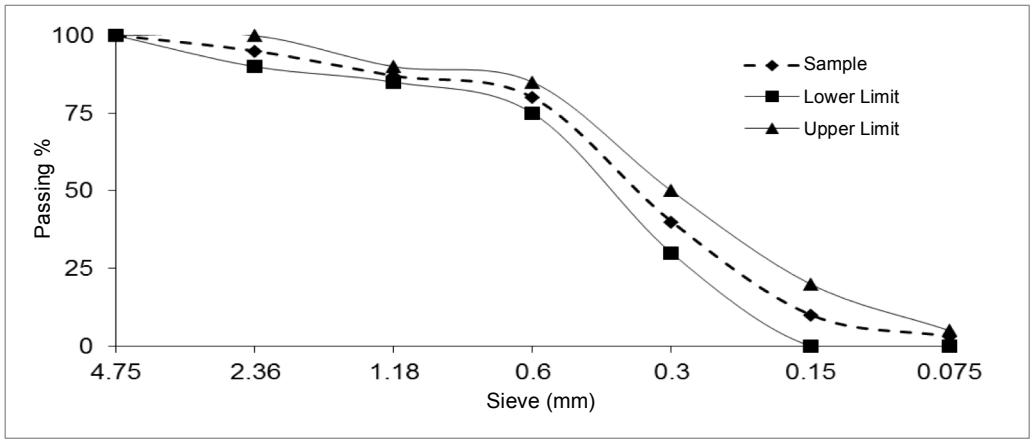

Figure 2. *Sand Grading - IDU 600-11 Specification Limits*

Table 7. *Results of chemical tests in cement*

Chemical Properties	*NTC-321 Requirement*	*Result*	*Verification*
MgO	*Max. 7%*	*0.91%*	*Complies*
SO_3	*Max.3.5%*	*2.3%*	*Complies*
Loss on ignition	*Max. 5%*	*1.16%*	*Complies*
Insoluble residue	*Max. 4%*	*1.25%*	*Complies*

Table 8. *Results of physical and mechanical tests in cement*

Chemical Properties	NTC-121 Requirement	Result	Verification
Fineness (Blaine)	280 m^2/kg	418	Complies
Retained in sieve No.325		1.11%	Complies
Expansion in autoclave	Max. 0.8%	0.003%	Complies
Vicat initial setting time	Min. 45 minutes	117 minutes	Complies
Vicat final setting time	Max. 8 hours	2.84 hours	Complies
Compressive strength at 3 days	Min. 12.5 MPa	28.7 MPa	Complies
Compressive strength at 7 days	Min. 19.5 MPa	38.5 MPa	Complies

Table 9. *Concrete Mix Design*

Material	Unit	Quantity
Cement type 1M	kg	400
Gravel	kg	1180
Sand	kg	686
Water	kg	170
Water reducer	kg	1.8
High-range plasticizer	kg	0.6
Total for $1m^3$		**2438.4**

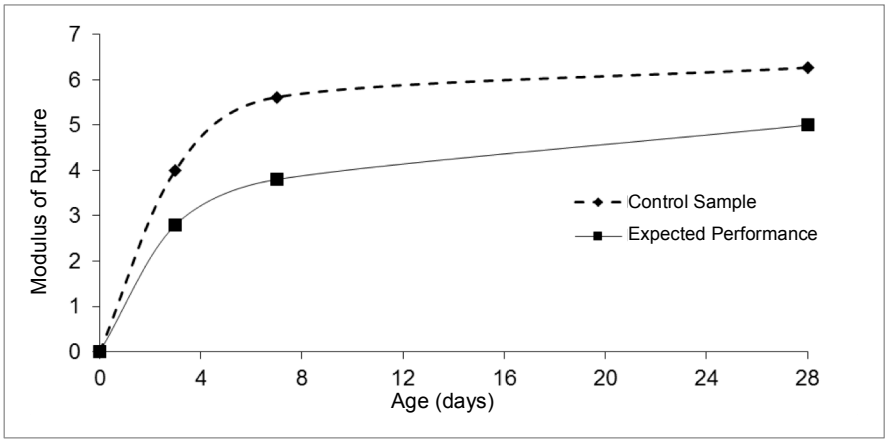

Figure 3. *Mix design verification*

3.2 Tests in the plastic state and mechanical tests in the hardened state

Table 10 shows the results of the tests in samples in the plastic state.

Whereas Table 11 shows the test results in the hardened state in cylinders of 150 mm diameter and 300 m height, and beams of 150 mm x 150 mm x 550 mm.

3.3 Fatigue tests

The results obtained during the fatigue tests in the specimens of 100 mm x 100 mm x 350 mm with different fiber quantities and the control sample are shown in Figures 4, 5, 6 and 7. The rupture stress for 1 loading cycle corresponds to that obtained in the specimens of 100 mm x 100 mm x 350 mm.

Table 10. *Test results for freshly mixed concrete*

Description	Slump (mm)	Air %	Unit Mass (kg/m³)
Control sample	125	1.55%	2372
Sample 20 kg/m³	125	2.00%	2342
Sample 40 kg/m³	100	2.70%	2412
Sample 80 kg/m³	90	4.95%	2351

Table 11. *Test results for hardened concrete*

Description	Compressive Strength at 7 Days (MPa)	Compressive Strength at 28 Days (MPa)	Modulus of Rupture at 7 Days (MPa)	Modulus of Rupture at 28 Days (MPa)	Modulus of Elasticity at 28 Days (MPa)
Control sample	52.61	65.81	5.61	6.26	23193
Sample 20 kg/m³	50.22	65.28	6.11	6.81	25551
Sample 40 kg/m³	50.45	65.31	6.34	7.05	27938
Sample 80 kg/m³	51.35	66.11	7.45	8.33	29745

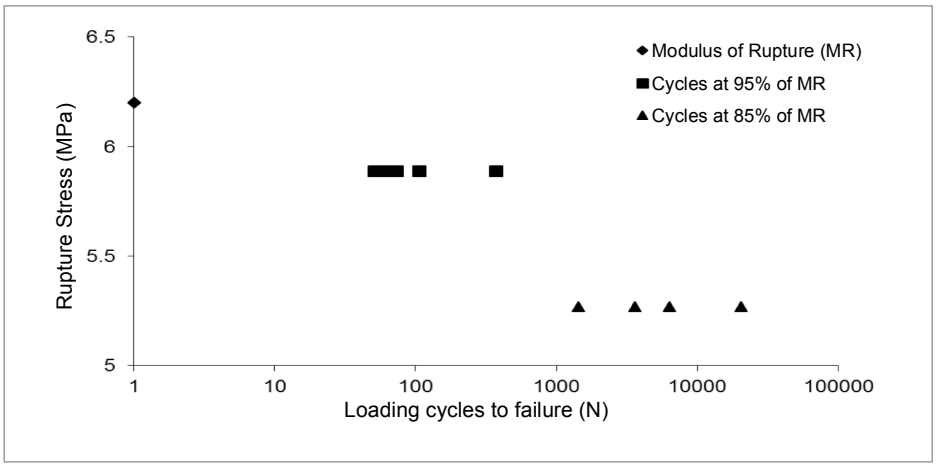

Figure 4. *Fatigue test results of control sample*

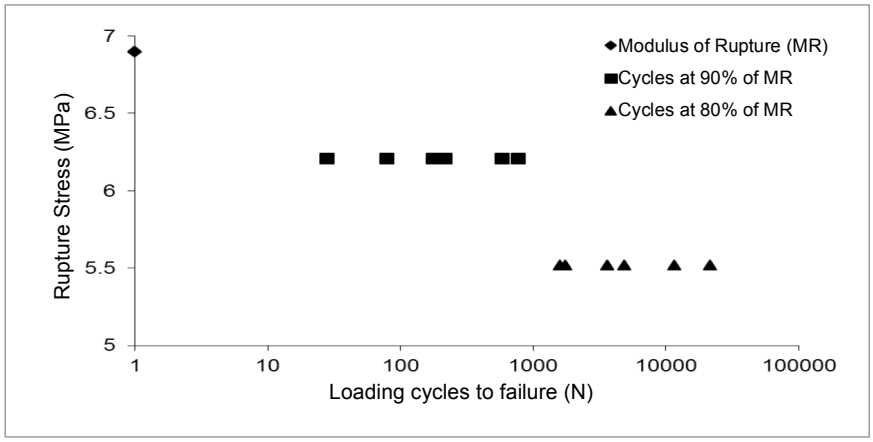

Figure 5. *Fatigue test results of sample with fiber content of 20 kg/m³*

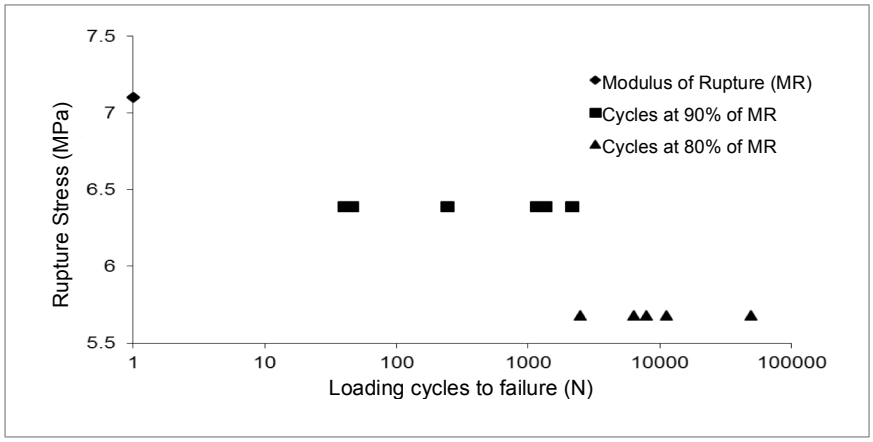

Figure 6. *Fatigue test results of sample with fiber content of 40 kg/m³*

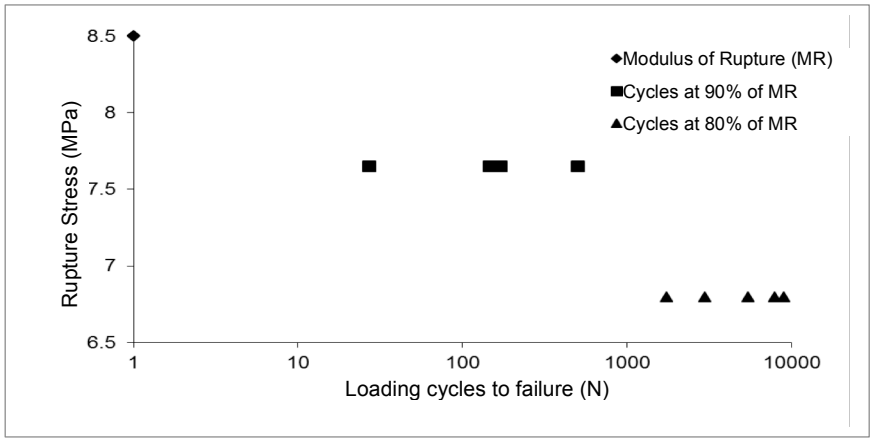

Figure 7. *Fatigue test results of sample with fiber content of 80 kg/m³*

3.4 Statistical analysis of the results

The parameters of the Weibull distribution α, μ and the prediction of the number of cycles with a 50%, 80% and 90% of failure probability for each rupture stress (n), is shown in Table 12.

Using this information, fatigue curves were graphed for each mixture using different failure probabilities. These curves are shown in Figures 8, 9, and 10, along with the best-fitted regression Equation.

.

Table 12. *Weibull parameters for each type of mix*

Sample	Rupture Stress (MPa)	α	μ	n (P_f 50%)	n (P_f 80%)	n (P_f 90%)
Control	6.20	0.976	131	1	1	1
	5.89			90	29	14
	5.27	0.92	7669	5149	1502	665
S 20 kg/m^3	6.90	1.033	311	1	1	1
	6.21			219	73	36
	5.52	0.959	7314	4992	1531	700
S 40 kg/m^3	7.10	0.963	819	1	1	1
	6.39			560	173	80
	5.68	0.789	13549	8515	2025	783
S 80 kg/m^3	8.50	1.043	215	1	1	1
	7.65			152	51	25
	6.80	1.823	6089	4981	2675	1773

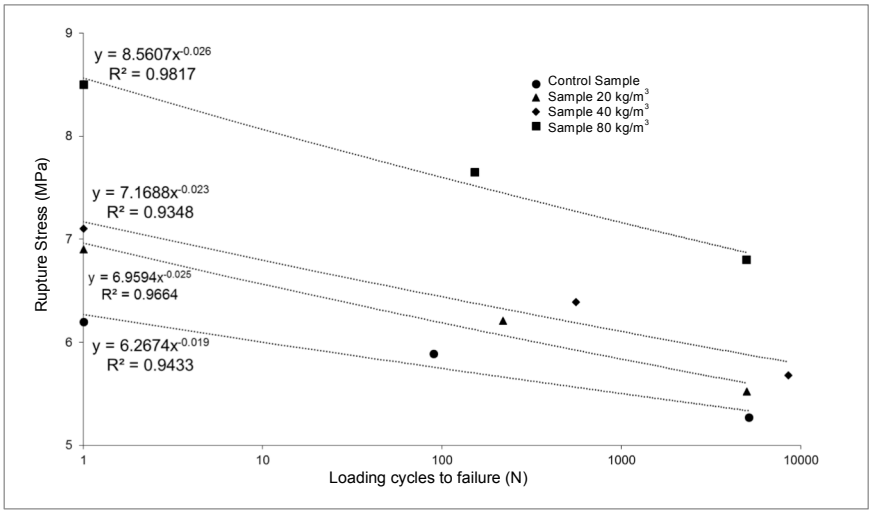

Figure 8. *Fatigue curves with 50% failure probability*

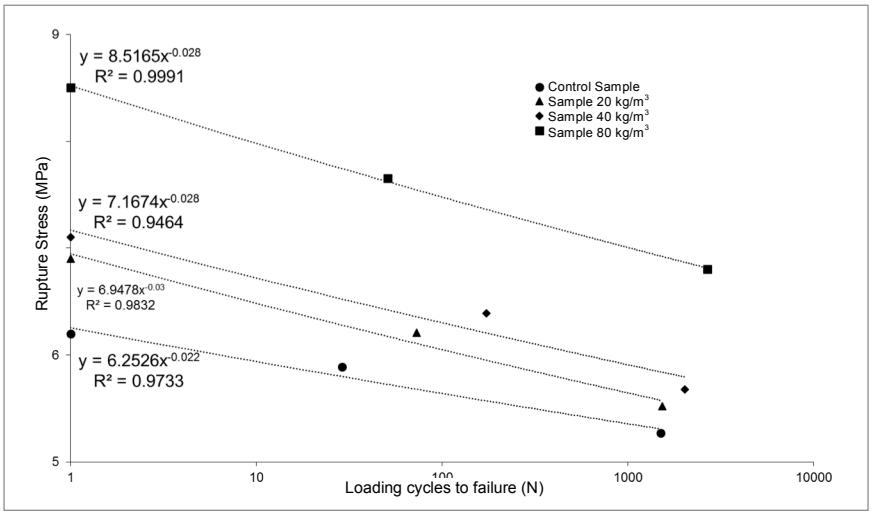

Figure 9. *Fatigue curves with 80% failure probability*

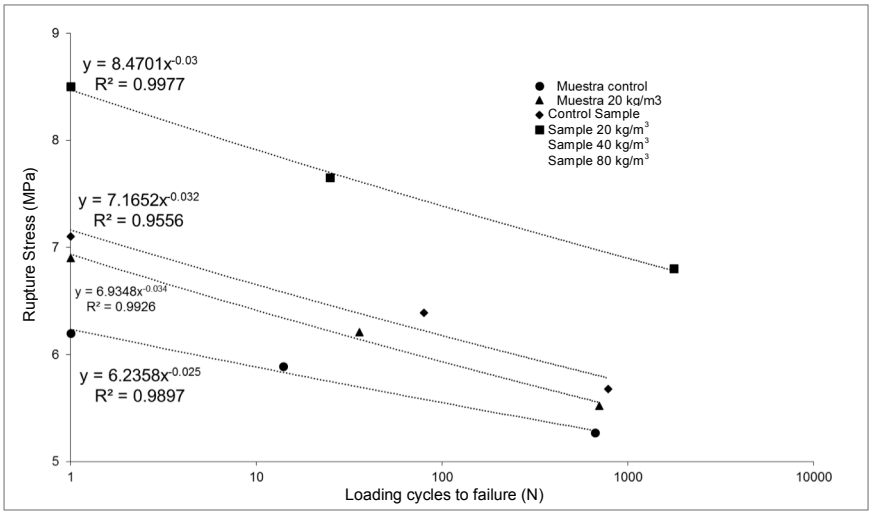

Figure 10. *Fatigue curves with 90% failure probability*

It is necessary to find the rupture stress for one million cycles (σ_6) and the slope of the fatigue curve (b), from each one of the curves. These parameters were obtained by applying the regression equation for one million loading cycles and taking the negative inverse of the exponent of the regression equation. The parameters obtained for each considered failure probability are shown in Table 13, 14 and 15. The column named σ_6 variation is the result of comparing the rupture stress for one million cycles (σ_6) of the mixtures with fibers, with the rupture stress for one million cycles (σ_6) of the control mix.

The average of the variation of the rupture stress for one million cycles (σ_6) of the mixtures with fibers compared with the control sample, is shown in Table 16.

This section of the paper will address the analysis of the results obtained in this research compared with results reported by researches with similar goals. Table 17 shows the equivalence between metal fiber contents in kg/m³ and in volume percentages. This conversion will be useful to compare results from different authors.

Table 13. *Parameters of the fatigue curves with 50% failure probability*

Sample	Fiber %	MR (MPa)	σ_6 (MPa)	b	-1/b	σ_6/MR	σ_6 Variation
Control sample	0.00%	6.20	4.82	-0.019	53	0.78	0%
Sample 20 kg/m³	0.25%	6.90	4.93	-0.025	40	0.71	2%
Sample 40 kg/m³	0.50%	7.10	5.22	-0.023	43	0.73	8%
Sample 80 kg/m³	1.00%	8.50	5.98	-0.026	38	0.70	24%

Table 14. *Parameters of the fatigue curves with 80% failure probability*

Sample	Fiber %	MR (MPa)	σ_6 (MPa)	b	-1/b	σ_6/MR	σ_6 Variation
Control sample	0.00%	6.20	4.61	-0.022	45	0.74	0%
Sample 20 kg/m³	0.25%	6.90	4.59	-0.03	33	0.67	0%
Sample 40 kg/m³	0.50%	7.10	4.87	-0.028	36	0.69	6%
Sample 80 kg/m³	1.00%	8.50	5.79	-0.028	36	0.68	25%

Table 15. *Parameters of the fatigue curves with 90% failure probability*

Sample	Fiber %	MR (MPa)	σ_6 (MPa)	b	-1/b	σ_6/MR	σ_6 Variation
Control sample	0.00%	6.20	4.42	-0.025	40	0.71	0%
Sample 20 kg/m³	0.25%	6.90	4.34	-0.034	29	0.63	-2%
Sample 40 kg/m³	0.50%	7.10	4.61	-0.032	31	0.65	4%
Sample 80 kg/m³	1.00%	8.50	5.60	-0.03	33	0.66	27%

Table 16. *Average of the σ_6 variation of the failure probabilities considered*

Sample	Fiber %	MR (MPa)	Average of σ_6 Variation
Control sample	0.00%	6.20	0%
Sample 20 kg/m^3	0.25%	6.90	0%
Sample 40 kg/m^3	0.50%	7.10	6%
Sample 80 kg/m^3	1.00%	8.50	25%

Table 17. *Equivalence between steel fiber contents*

Sample	Volume Percentage (%)
Control sample	0.00%
S 20 kg/m^3	0.25%
S 40 kg/m^3	0.50%
S 80 kg/m^3	1.00%

First, results obtained from the measurements of the material's basic properties in the plastic and hardened states are analyzed, and then, the results of the fatigue curves. The analysis is based on curves reported by other researchers, whose parameters used the rational French design method to characterize fatigue curves of cementitious materials, rupture stress for one million cycles (σ_6), and slope of the fatigue law (b).

The slump of concrete mixes showed a decrease of 25 mm for a fiber content of 40 kg/m^3 (0.5%) and 35 mm in the mix with 80 kg/m^3 (1.0%); the latter is consistent with the slump decrease reported by Jun and Stang (1998), who worked with the same steel fiber content. In general, slump losses found in this research are within the reduction range reported by ACI 544.1R (2009), which mentions that the incorporation of steel fibers between 0.25% and 1.5% will reduce slump between 25 mm and 102 mm

Air content measurements show that concrete mixes reinforced with steel fibers increase the air content as metal fibers are incorporated, which is consistent with the reports of ACI 544.1R (2009).

The compressive strength results do not show a significant variation in concrete mixes with different fiber contents, which confirms studies by different authors (ACI Committee 544, 2009; Bentur and Sidney, 2007; Goel et al., 2012; Grzybowski and Meyer, 1993; Huang and Zhao, 1995; Jun and Stang, 1998; Lee and Barr, 2004; Naaman and Hammoud, 1998; Singh and Kaushik, 2000; Singh et al., 2005).

The modulus of rupture increased with the incorporation of steel fibers by 9% for a fiber content of 20 kg/m^3 (0.25%), 13% in the mix with 40 kg/m^3 (0.5%), and 33% in the mix with 80 kg/m^3 (1.0%), compared with the control mix. These figures are within the range of increases of the modulus of rupture between 10% and 35% for fiber contents between 0.5% and 1%, found by Johnston and Zemp (1991), Huang and Zhao (1995), Jun and Stang (1998), Naaman and Hammoud (1998), Singh et al. (2005) and Goel et al. (2012).

The elasticity modulus measured in this research increased by 10% for the mix with 20 kg/m^3 (0.25%), 20% in the mix with 40 kg/m^3 (0.5%), and 28% in the mix with 80 kg/m^3 (1.0%), compared with the control mix. According to ACI 544.1R, under 2% of fiber, the elasticity modulus does not increase significantly. However, ACI 544.1R (2009) does not indicate the orders of magnitude of the elasticity modulus.

The average fatigue life variation in the considered failure probabilities indicates that the fatigue life does not increase in the mix with fiber content of 20 kg/m^3 (0.25%), while it does increase by 6% for the mix with 40 kg/m^3 (0.5%) and 25% in the mix with 80 kg/m^3 (1.0%), compared with the control mix. These results show the effect of incorporating steel fibers on the concrete's fatigue life, which entails a better performance under cyclic loads when the steel fiber content is higher than 40 kg/m^3 (0.5%).

As mentioned earlier in the theoretical framework, the comparison made with data reported by different publications is focused on knowing the orders of magnitude and the trends of the fatigue curves, because in the absence of a universal test standard to measure fatigue, test conditions differ from one research to another. Among these differences, the following should be highlighted: load types, dimensions of tested specimens, fiber type, fiber quantities, modulus of rupture of concrete, and the range of stresses applied for measuring fatigues.

The parameters that characterize the fatigue curves in the French rational method (stresses for one million cycles (σ_6), and the slope of the fatigue law (b), were calculated with published data. Regarding concretes without fibers, Table 18 shows the results taken from the references (Goel et al., 2012; Johnston and Zemp, 1991; Oh, 1991; Shi et al., 1993).

It can be observed that the rupture stress for one million cycles (σ_6) is higher than that reported by quoted references. However, if divided among the modulus of rupture, it is evidenced that results are similar. Table 19 shows the results taken from the references for concretes reinforced with steel fiber contents of 40 kg/m^3 (0.5%) (Goel et al., 2012; Singh and Kaushik, 2003).

Table 18. *Properties of fatigue curves of mixes without fibers*

Author	Range Evaluated in Stress Ratios (σ_6/MR)		MR (MPa)	σ_6 (MPa)	b	-1/b	σ_6/MR
Byung Hwan, 1991	65%	85%	4.54	2.80	-0.052	20	0.62
Johnston et al., 1991	80%	90%	4.45	3.20	-0.040	25	0.72
Shi et al., 1993	65%	90%	6.04	3.50	-0.042	24	0.58
Goel et al., 2012	65%	90%	4.89	3.10	-0.045	23	0.63
LCPC-SETRA, 1997 (Class 5)				2.15	-0.063	16	
LCPC-SETRA, 1997 (Class 4)				1.95	-0.067	15	
LCPC-SETRA, 1997 (Class 3)				1.63	-0.067	15	
LCPC-SETRA, 1997 (Class 2)				1.37	-0.071	14	
PCA, 1984	45%	100%					0.50
Control sample - P_f 50%	**85%**	**95%**	**6.20**	**4.82**	**-0.019**	**53**	**0.78**
Control sample - P_f 80%	**85%**	**95%**	**6.20**	**4.61**	**-0.022**	**45**	**0.74**
Control sample - P_f 90%	**85%**	**95%**	**6.20**	**4.42**	**-0.025**	**40**	**0.71**

Table 19. *Properties of fatigue curves of mixes with 0.5% fiber*

Author	Range Evaluated in Stress Ratios (σ_6/MR)		MR (MPa)	Fiber %	σ_6 (MPa)	b	-1/b	σ_6/MR
Singh et al., 2000	60%	90%	5.74	0.5%	4.30	-0.028	36	0.75
Goel et al., 2012	65%	90%	6.08	0.5%	4.00	-0.047	22	0.66
M 40 kg/m³ - P_f 50%	**80%**	**90%**	**7.10**	**0.5%**	**5.22**	**-0.023**	**43**	**0.73**
M 40 kg/m³ - P_f 80%	**80%**	**90%**	**7.10**	**0.5%**	**4.87**	**-0.028**	**36**	**0.69**
M 40 kg/m³ - P_f 90%	**80%**	**90%**	**7.10**	**0.5%**	**4.61**	**-0.032**	**31**	**0.65**

It is evidenced that the value of σ_6 found experimentally in this research is higher than the values reported by Singh and Kaushik (2003) and Goel et al. (2012). However the σ_6/MR ratios are similar.

For 1% steel fiber contents, Table 20 shows data taken from the references (Goel et al., 2012; Huang and Zhao, 1995; Johnston and Zemp, 1991; Jun and Stang, 1998; Singh and Kaushik, 2003; Singh et al., 2005), which show that the orders of magnitudes of the σ_6/MR ratios are similar.

Table 20. *Properties of fatigue curves of mixes with 1.0% fiber*

Author	Range Evaluated in Stress Ratios (σ_6/MR)		MR (MPa)	Fiber %	σ_6 (MPa)	b	-1/b	σ_6/MR
Singh et al., 2000	60%	90%	5.74	0.5%	4.30	-0.028	36	0.75
Goel et al., 2012	65%	90%	6.08	0.5%	4.00	-0.047	22	0.66
Johnston et al., 1991	80%	90%	7.03	1.0%	4.90	-0.032	32	0.70
Chenkui et al., 1995	65%	90%	5.99	1.0%	3.80	-0.050	20	0.63
Jun & Stang, 1998	80%	95%	6.73	1.0%	4.50	-0.022	46	0.67
Singh et al., 2000	60%	90%	6.67	1.0%	4.60	-0.036	28	0.69
Singh et al., 2005	70%	90%	7.61	1.0%	5.80	-0.027	38	0.76
Singh et al., 2005	70%	90%	7.50	1.0%	5.60	-0.031	33	0.75
Singh et al., 2005	70%	90%	7.46	1.0%	5.70	-0.028	36	0.76
Goel et al., 2012	65%	90%	7.18	1.0%	5.10	-0.041	25	0.71
M 80 kg/m³ - P_f 50%	**80%**	**90%**	**8.50**	**1.0%**	**5.98**	**-0.026**	**38**	**0.70**
M 80 kg/m³ - P_f 80%	**80%**	**90%**	**8.50**	**1.0%**	**5.79**	**-0.028**	**36**	**0.68**
M 80 kg/m³ - P_f 90%	**80%**	**90%**	**8.50**	**1.0%**	**5.60**	**-0.030**	**33**	**0.66**

4. Conclusions

The incorporation of steel fibers in concrete for pavements does not increase the fatigue life for fiber contents of 20 kg/m³ (0.25%), while it does increase by 6% with 40 kg/m³ (0.5%) and 25% with 80 kg/m³ (1.0%), compared with concrete without fibers, on average.

The slopes of fatigue curves increase when reinforcing concrete with steel fibers. Were it not for the increase of the modulus of rupture of concrete by the incorporation of steel fibers, the fatigue life would not show improvements compared with the control mix.

The variation coefficients of data obtained in the fatigue tests are on average 100%; therefore, it is highly relevant to use the Weibull probability distribution for processing the fatigue test results, which, in this research, provided fatigue curves with regression coefficients over 0.90. It is important to mention that the regression coefficients increased as the failure probability increased.

5. References

ACI Committee 360. (2006), Design of slabs-on-ground.

ACI Committee 544. (2009), State-of-the-Art Report on Fiber Reinforced Concrete (70). ACI Journal Proceedings.

Batson G., Ball C., Bailey L., Landers E. and Hooks J. (1972), Flexural fatigue strength of steel fiber reinforced concrete beams. ACI Journal Proceedings, 69(11), 673-677.

Bentur A. and Sidney M. (2007), Fibre Reinforced Cementitious Composites (2a Edición.). Canadá: Taylor y Francis.

Cervo T. C. (2004), Estudo da resistência à fadiga de concretos de cimento Portland para pavimenta\ccão (Tesis doctoral). Universidade de São Paulo, São Paulo.

Goel S., Singh S. and Singh P. (2012), Fatigue Analysis of Plain and Fiber-Reinforced Self-Consolidating Concrete. ACI Materials Journal, 109(5), 573-582.

Grzybowski M. and Meyer C. (1993), Damage accumulation in concrete with and without fiber reinforcement. ACI Materials Journal, 90(6), 594-604.

Hsu T. T. (1981), Fatigue of plain concrete. In ACI Journal Proceedings, 78(4), 292-305.

Huang C. and Zhao G. (1995), Properties of steel fibre reinforced concrete containing larger coarse aggregate. Cement and Concrete Composites, 17(3), 199–206.

Huang Yang (2004), Pavement analysis and design. New Jersey, United States of America: Prentice-Hall, Pearson.

Johnston C. D. and Zemp R. W. (1991), Flexural Fatigue Performance of Steel Fiber Reinforced Concrete–Influence of Fiber Content, Aspect Ratio, and Type. ACI materials Journal, 88(4), 375-383.

Jun Z. and Stang H. (1998), Fatigue performance in flexure of fiber reinforced concrete. ACI Materials Journal, 95(1), 58-67.

LCPC. (1997), Conception et dimensionnement des structures de chaussee (Guide technique.).

Lee M. K. and Barr B. I. G. (2004), An overview of the fatigue behaviour of plain and fibre reinforced concrete. Cement and Concrete Composites, 26(4), 299–305.

Li H., Zhang M. and Ou J. (2007), Flexural fatigue performance of concrete containing nano-particles for pavement. International Journal of Fatigue, 29(7), 1292–1301.

Li Z. (2011), Advanced concrete technology. Hoboken, United States of America: John Wiley y Sons.

Lv Y., Cheng H. and Ma Z. (2012), Fatigue performances of glass fiber reinforced concrete in flexure. Procedia Engineering, 31(1), 550–556.

Meda A. and Plizzari G. A. (2004), New design approach for steel fiber-reinforced concrete slabs-on-ground based on fracture mechanics. ACI Structural Journal, 101(3), 298-303.

Mehta P. K. and Monteiro P. J. (2006), Concrete: microstructure, properties, and materials (3a edición). Recuperado de https://www.researchgate.net/file.PostFileLoader.html?id=554a654dd4c118f1798b458ayassetKey=AS%3A273670184865796%401442259465245.

MEPDG A. (2007), Guide for the mechanistic-empirical design of new and rehabilitated pavement structures. Inc, ERES Consultants Division.

Ministerio Ambiente, Vivienda and Desarrollo Territorial (2010), Reglamento Colombiano de Construcción sismo resistente. NSR-10. Bogotá D.C.

Naaman A. and Hammoud H. (1998), Fatigue characteristics of high performance fiber-reinforced concrete. Cement and Concrete Composites, 20(5), 353–363.

Oh B. H. (1991), Fatigue life distributions of concrete for various stress levels. ACI Materials Journal, 88(2), 122–128.

Packard R. G. (1984), Thickness design for concrete highway and street pavements. Recuperado de https://ceprofs.civil.tamu.edu/dzollinger/CVEN-637-Fall%202004/EB109.PDF.

Papagiannakis A. and Masad E. A. (2008), Pavement design and materials. Hoboken, United States of America: John Wiley y Sons

Reyes F. A. (2003), Diseño racional de pavimentos (1a edición.). Bogotá, Colombia: CEJA Centro editorial Javeriano.

Shi X., Fwa T. and Tan S. (1993), Flexural fatigue strength of plain concrete. ACI Materials Journal, 90(5), 435-440.

Singh S. and Kaushik S. (2000), Flexural fatigue life distributions and failure probability of steel fibrous concrete. ACI Materials Journal, 97(6), 658–667.

Singh S. and Kaushik S. (2003), Fatigue strength of steel fibre reinforced concrete in flexure. Cement and Concrete Composites, 25(7), 779–786.

Singh S. Mohammadi Y. and Kaushik S. (2005), Flexural fatigue analysis of steel fibrous concrete containing mixed fibers. ACI materials journal, 102(6), 438-444.

Vassilopoulos A. P. (2010), Fatigue life prediction of composites and composite structures (CRC Press.). Washington D.C., United States of America: Woodhead publishing limited.